Dynamics of myosin, microtubules, and Kinesin-6 at the cortex during cytokinesis in *Drosophila* S2 cells

Ronald D. Vale,[1,2] James A. Spudich,[1,3] and Eric R. Griffis[1,2]

[1]Physiology Course, Marine Biological Laboratory, Woods Hole, MA 02543
[2]Howard Hughes Medical Institute and Department of Cellular and Molecular Pharmacology, University of California, San Francisco, CA 94158
[3]Department of Biochemistry, Stanford University Medical Center, Stanford, CA 94305

Signals from the mitotic spindle during anaphase specify the location of the actomyosin contractile ring during cytokinesis, but the detailed mechanism remains unresolved. Here, we have imaged the dynamics of green fluorescent protein–tagged myosin filaments, microtubules, and Kinesin-6 (which carries activators of Rho guanosine triphosphatase) at the cell cortex using total internal reflection fluorescence microscopy in flattened *Drosophila* S2 cells. At anaphase onset, Kinesin-6 relocalizes to microtubule plus ends that grow toward the cortex, but refines its localization over time so that it concentrates on a subset of stable microtubules and along a diffuse cortical band at the equator. The pattern of Kinesin-6 localization closely resembles where new myosin filaments appear at the cortex by de novo assembly. While accumulating at the equator, myosin filaments disappear from the poles of the cell, a process that also requires Kinesin-6 as well as possibly other signals that emanate from the elongating spindle. These results suggest models for how Kinesin-6 might define the position of cortical myosin during cytokinesis.

Introduction

After the separation of sister chromatids, cell division is completed by the formation and invagination of an actomyosin contractile ring (the cleavage furrow) that separates the cell in two. Numerous genetic screens have identified the small GTPase RhoA as a master regulator of the machinery that drives cleavage furrow formation (for reviews see Piekny et al., 2005; Eggert et al., 2006; Miller et al., 2008). In its GTP-bound state, RhoA activates Rho kinase, which results in downstream myosin filament formation and ATPase activation, stimulation of formins to induce actin polymerization, and activation of anillin as a scaffold for myosin, RhoA, septins, and other proteins. Deletion of RhoA blocks cytokinesis, and reporters for the GTP form of RhoA reveal that Rho activity increases at anaphase at the site of cleavage furrow formation (Yoshizaki et al., 2003; Bement et al., 2005; Canman et al., 2008).

An important question that remains to be answered is how activation of Rho becomes restricted to the cell equator. Many studies have shown that spindle microtubules play an important "instructive" role in defining the zone of Rho activation. Classical studies by Rappaport involving the micromanipulation of mitotic spindles in echinoderm eggs demonstrated that microtubules specify the location of the cleavage furrow (Rappaport, 1971). More recent work has shown that myosin-based contractility (a result of Rho activation) increases at anaphase, but when microtubules are depolymerized, this contractility occurs randomly throughout the cortex and is not focused at the equatorial zone (Canman et al., 2000; Murthy and Wadsworth, 2008). A particularly intriguing subset of microtubules is stabilized at the cortex near the site of furrow formation, and these microtubules might mark the site for contractile ring formation (Canman et al., 2003; Foe and von Dassow, 2008). In addition, bundled microtubules that form between the separating chromosomes in the interior (referred to here as the "central spindle") appear to be endowed with the capability of triggering the formation of a cleavage furrow (Inoue et al., 2004; Bringmann and Hyman, 2005). However, the microtubule-based signaling mechanism also appears to be robust to spindle geometry, as furrows will form in cells with monopolar spindles that lack overlapping microtubules (Canman et al., 2003; Hu et al., 2008).

Correspondence to Eric Griffis: griffis@cmp.ucsf.edu

Abbreviations used in this paper: Con A, concanavalin A; dsRNA, double-stranded RNA; MT, microtubule; Pav, Pavarotti; TIRF, total internal reflection fluorescence.

The Rockefeller University Press $30.00
J. Cell Biol. Vol. 186 No. 5 727–738
www.jcb.org/cgi/doi/10.1083/jcb.200902083

Supplemental Material can be found at:
http://jcb.rupress.org/cgi/content/full/jcb.200902083/DC1

One way in which microtubules could specify the localization of the cleavage furrow is by transporting Rho "activators" to the equator. A motor protein that likely links microtubules to Rho activation is Kinesin-6 (Pavarotti [Pav] in *Drosophila*, Zen-4 in *Caenorhabditis elegans*, and MKLP1 in mammals), which is required for cytokinesis in many organisms from *Dictyostelium discoideum* to mammals (for reviews see D'Avino et al., 2005; Piekny et al., 2005; Glotzer, 2009). Kinesin-6 bundles microtubules in the central spindle and is localized to microtubules at the equatorial cortex (Minestrini et al., 2003; Nishimura and Yonemura, 2006). Kinesin-6 interacts with two important regulators of small GTPases: a GTPase-activating protein (GAP; CYK4 in *C. elegans*, RacGAP50C in *Drosophila*, and MgcRacGAP in mammals) with which it forms a heterotetrameric complex, and a GEF protein (Pebble in *Drosophila* and Ect2 in other organisms) that interacts with the GAP (Glotzer, 2009). The GAP protein reduces Rac activity (Yoshizaki et al., 2003; Canman et al., 2008) and promotes nucleotide flux of Rho (Miller and Bement, 2009) at the equator, and the GEF exchanges nucleotide to convert Rho to an active GTP-bound state (Somers and Saint, 2003; Kamijo et al., 2006). The exact mechanism of how Kinesin-6 restricts the activation of Rho to the equator is not understood, although a recent computer model has suggested how equatorial activation might arise from a difference in microtubule stability at the equator versus the poles (Odell and Foe, 2008).

In addition to the "stimulatory Rho" signals that stable microtubules might send to the equator, dynamic microtubules reaching the poles were proposed to send an "inhibitory Rho" signal that helps to sharpen the position of the furrow. In support of this idea, nocodazole-mediated depolymerization of dynamic astral microtubules tends to defocus the "cleavage furrow zone" (Foe and von Dassow, 2008; Murthy and Wadsworth, 2008). However, the molecular basis of reducing myosin activity at the poles (also known as cortical relaxation) is not understood.

To better understand the signaling mechanisms by which microtubules mark the cortex for contractile ring formation, we have used dual color, total internal reflection fluorescence (TIRF) microscopy to image myosin, microtubules, and Kinesin-6 at the cortex at the onset of cytokinesis (metaphase-to-anaphase transition) in *Drosophila* S2 cells. At the start of anaphase in cells with bipolar spindles, we show that myosin filaments suddenly appear at the equator and disappear from the poles as the chromosomes/centrosome move apart during spindle elongation. In monopolar spindles, the converse pattern occurs, as myosin disappears from the central region of the cortex (chromosomes move toward the center in monopolar spindles) and appears at the surrounding peripheral cortex. These patterns of myosin localization closely resemble those of Kinesin-6, which is delivered to the cortex on microtubule tips at anaphase and then refines its localization to a subset of microtubules and along the cell cortex in the zone of myosin accumulation. Our live cell imaging of Kinesin-6–depleted cells also shows that this motor is involved in both equatorial accumulation and polar loss of myosin, which supports a hypothesis that it focuses the contractile ring through the delivery/sequestration of Rho activators at the equator.

Results

Myosin filaments relocalize to the equator without undergoing cortical flow

In previous work, we imaged myosin through mitosis and cytokinesis by wide-field imaging in *Drosophila* S2 cells stably expressing GFP fused to the myosin regulatory light chain (herein referred to as myosin-GFP; Dean et al., 2005). However, the out-of-focus fluorescence impaired our ability to obtain detailed information on cortical myosin at early stages of cytokinesis, and hence we turned to TIRF microscopy to visualize myosin just at the cell cortex. When S2 cells are plated on glass or plastic, the mitotic cells adhere poorly to the surface and round up; as a result, cortical myosin and microtubules cannot be imaged well by TIRF microscopy (unpublished data). To improve imaging, we plated cells on concanavalin A (Con A)-coated glass-bottom dishes, to which they adhere tightly and spread (Fig. 1 A; Rogers et al., 2002). Under these tightly adherent conditions, myosin is properly localized to the midzone, but the furrow cannot ingress and cells cannot complete cytokinesis (Goshima and Vale, 2003). However, this preparation enabled clear visualization of myosin at the cortex–coverslip interface during the early phase of cytokinesis after anaphase onset (Fig. 1 B). When visualized by TIRF, myosin-GFP appeared as small rods (Fig. 1 B, insets). With improved resolution offered by structured illumination TIRF microscopy, such rods appeared as "dumbbells" of two closely spaced GFP dots (unpublished data). Because GFP is localized at the motor domain at the ends of myosin thick filaments, we believe that the small rods seen by TIRF microscopy correspond to individual myosin thick filaments (note that the longer myosin filaments in *D. discoideum* are resolved as "dumbbells" by conventional TIRF microscopy; Yumura et al., 2008; unpublished data).

Changes in myosin localization at the cortex during anaphase are shown in Fig. 1 B. Just before anaphase, myosin filaments were found throughout the cortex, but were often absent from the center of the cortical footprint (in approximately the same position relative to the overlying mitotic spindle). Myosin filaments could be seen appearing and disappearing from the cortex during metaphase, indicating that they are dynamic. Although it was difficult to track individual myosin filaments with confidence for extended periods of time, many individual myosin filaments that could be tracked were associated with the cortex for relatively long periods of time (0.5–3 min). After the onset of anaphase, myosin filaments disappeared rapidly from the cortical surface at the poles (opposite ends of the cell defined by the mitotic spindle axis) and abruptly appeared at the equator; the equatorial increase often occurred first at the lateral regions and then subsequently filled into the center (Fig. 1 B). In some cells at very early anaphase, myosin also accumulated in localized "flares" outside of the equatorial zone, but these were not maintained and the majority of myosin ultimately stabilized on the cortex underlying the central spindle (unpublished data). Notably, we did not observe myosin filaments moving along the cortex from the poles to the equator; most filaments remained relatively stationary or displayed short (<1 μm) movements (Fig. 1 B and Video 1). Attachment to the Con A surface is unlikely to inhibit cortical flow per se because pronounced retrograde flow of myosin-GFP filaments occurs in adjacent interphase S2 cells

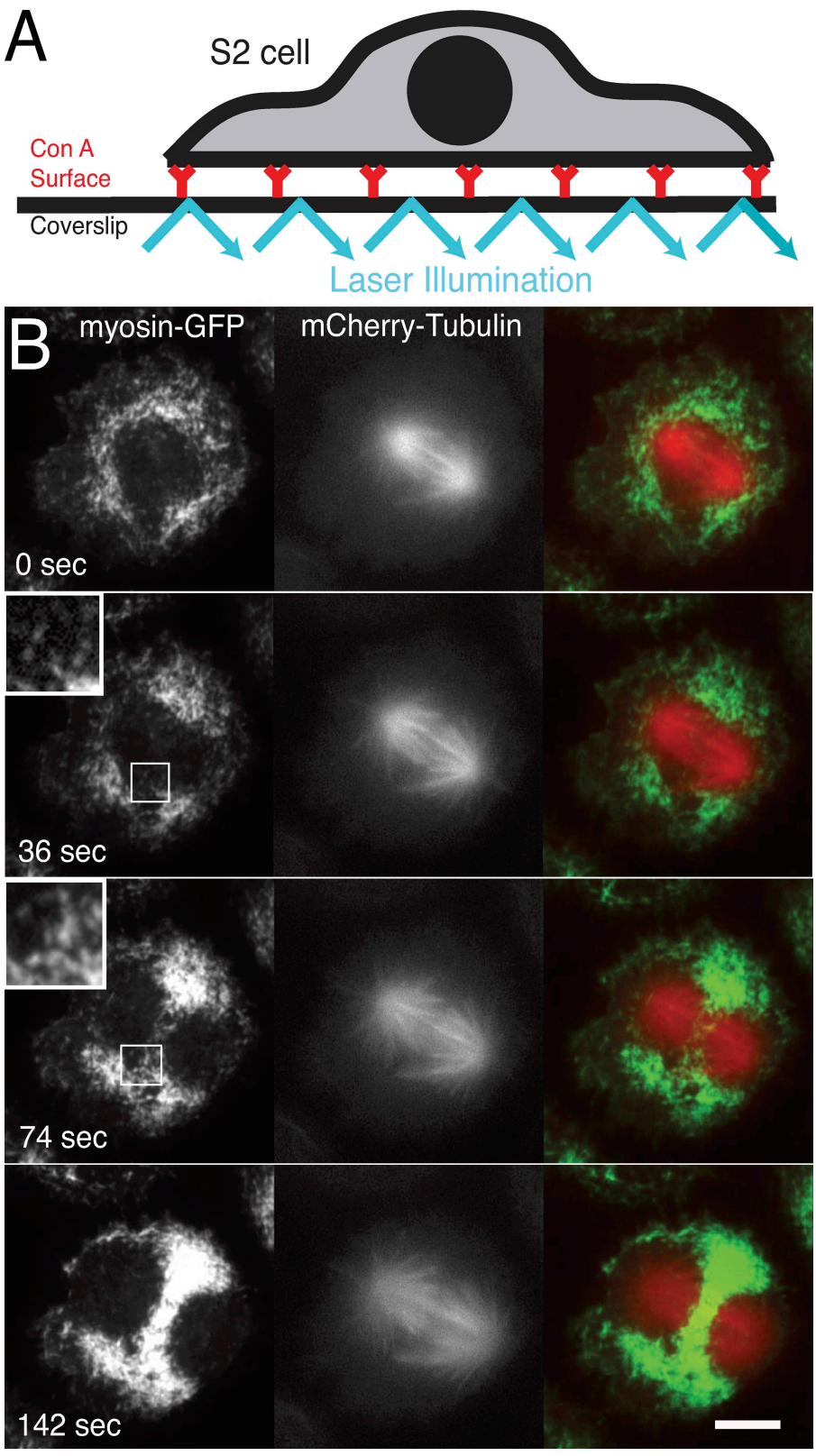

Figure 1. **Redistribution of myosin-GFP during anaphase in *Drosophila* S2 cells as observed by TIRF microscopy.** (A) A schematic diagram showing the experimental system of a *Drosophila* S2 cells adsorbed onto a Con A–coated coverslip and imaged using total internal reflection laser illumination. (B) A time sequence showing myosin-GFP imaged by TIRF (left), mCherry-tubulin imaged by wide field fluorescence (center), and a merge of the two images (right). The insets at 36 and 74 sec show enlarged views of a region at the equator where individual myosin rods (likely bipolar filaments) suddenly appear during early anaphase. For dynamics, see Video 1. Bar, 10 µm.

attached to the same surfaces (e.g., Videos 1–3). Late anaphase cells also often showed retrograde movement of myosin filaments at the periphery (unpublished data). We also imaged actin-GFP and Diaphanous-GFP (a formin in *Drosophila*; the main actin-nucleating protein during cytokinesis; Rogers et al., 2003; Watanabe et al., 2008) and found that both were rapidly recruited to the equator, as visualized by TIRF microscopy (Fig. S1).

Quantitative analysis revealed several features of the relocalization of myosin at anaphase. First, the total myosin-GFP intensity over the entire cortical footprint in the TIRF field increased

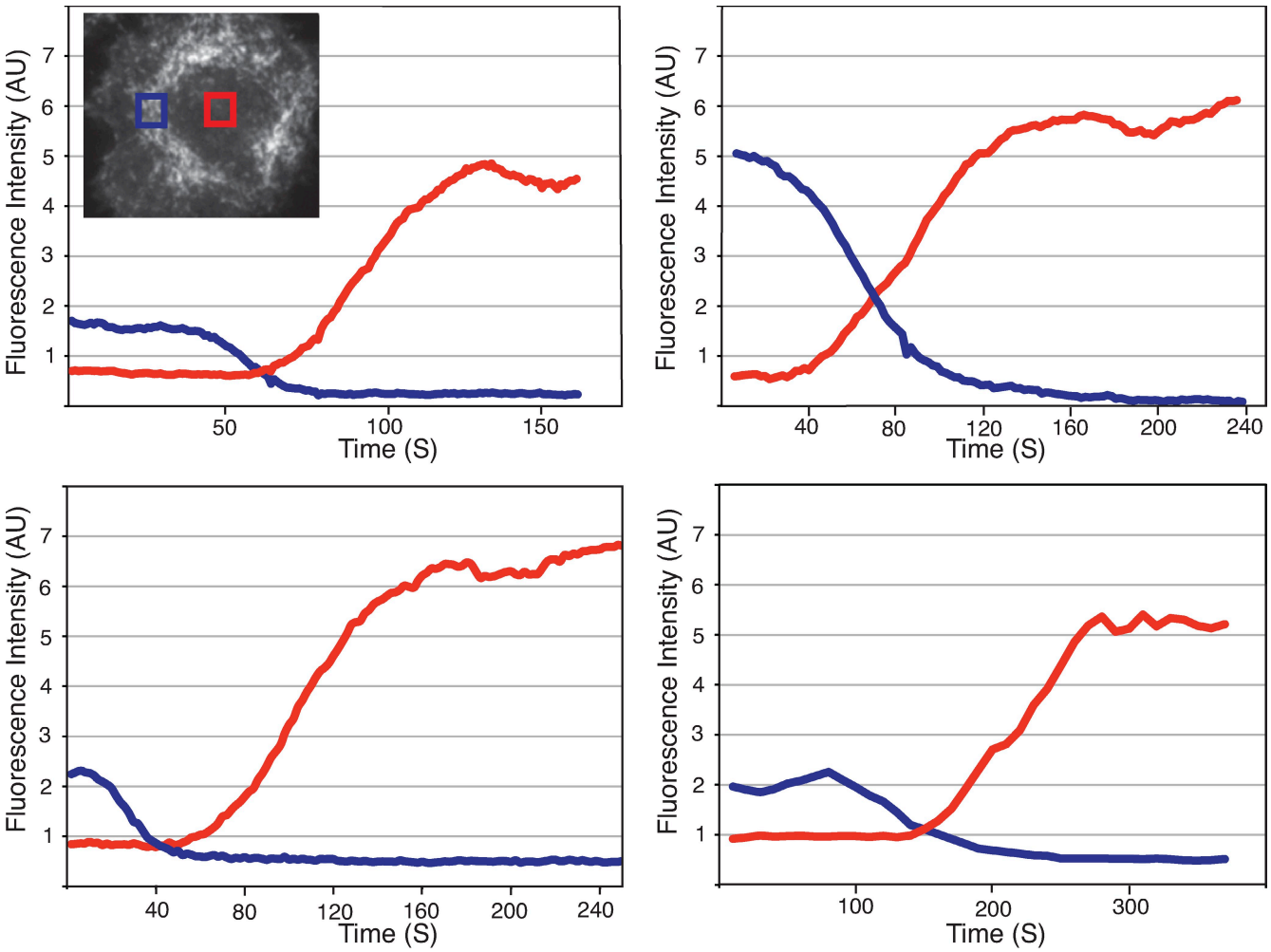

Figure 2. **Time course of myosin increase at the equator (red) and decrease at one of the poles (blue) in four representative cells.** Using ImageJ, a 3.17 × 3.17-µm area (boxes shown in the inset) was measured for its mean intensity over time at the cell equator or the pole over an image stack. Background intensity in a nearby area outside of the cell was subtracted from the above measurement. Fluorescence intensity is in arbitrary units.

between metaphase and anaphase (1.6 ± 0.3-fold, mean ± SD; $n = 7$). Although there was cell-to-cell variability, the disappearance of myosin from the polar regions generally preceded the appearance of myosin at the equatorial cortex (Fig. 2). The fluorescence intensity of GFP-myosin decreased at the poles by 7.2 ± 2.7-fold (mean ± SD; 18 measurements from an ∼10-µm^2 area from $n = 10$ cells) and preceded the increase in myosin-GFP at the equator (9.7 ± 5.3-fold; mean ± SD; $n = 10$ cells), with the half-maximal change in intensity occurring 65 ± 28 s earlier at the poles than the equator (mean ± SD; $n = 9$ cells). The loss of myosin usually occurred progressively from more central regions to more peripheral "polar" regions of the cortex, following a similar "path" as spindle elongation and chromosome movement during anaphase (Videos 1–3). When observing single filaments, many decreased their fluorescence intensity over several seconds and not instantaneously, reflecting filament disassembly and/or movement out of the evanescent field (Fig. S2).

In conclusion, for Con A–adhered S2 cells, myosin does not relocalize to the equator by cortical flow, but rather by the discrete disappearance and appearance of myosin filaments from the poles and equator, respectively. Myosin relocalization could be accomplished by nondynamic myosin filaments moving from the polar cortex into the cell interior (without any lateral movement in the TIRF field), with them then being transported internally to the spindle midzone (invisible in our TIRF field) and finally translocating vertically to the equatorial cortex. However, this possibility seems unlikely because the relocation of preexisting myosin filaments from the poles to the equator cannot solely account for the total increase in equatorial myosin, and because there are no "vertical" microtubule tracks that extend perpendicularly from the spindle midzone to the cortex. Hence, we favor the model that myosin filaments are disassembled at the poles and that equatorial myosin filaments form de novo through Rho-dependent activation of myosin filament assembly from soluble dimers.

Imaging of microtubules at the cortex during anaphase onset

We next sought to correlate the behavior of myosin and microtubules at the cell cortex in cell lines stably expressing myosin-GFP and mCherry–α-tubulin using TIRF microscopy. During metaphase, only the very tips of microtubules were visible at the cortex and were seen mostly in the center of the cortical footprint

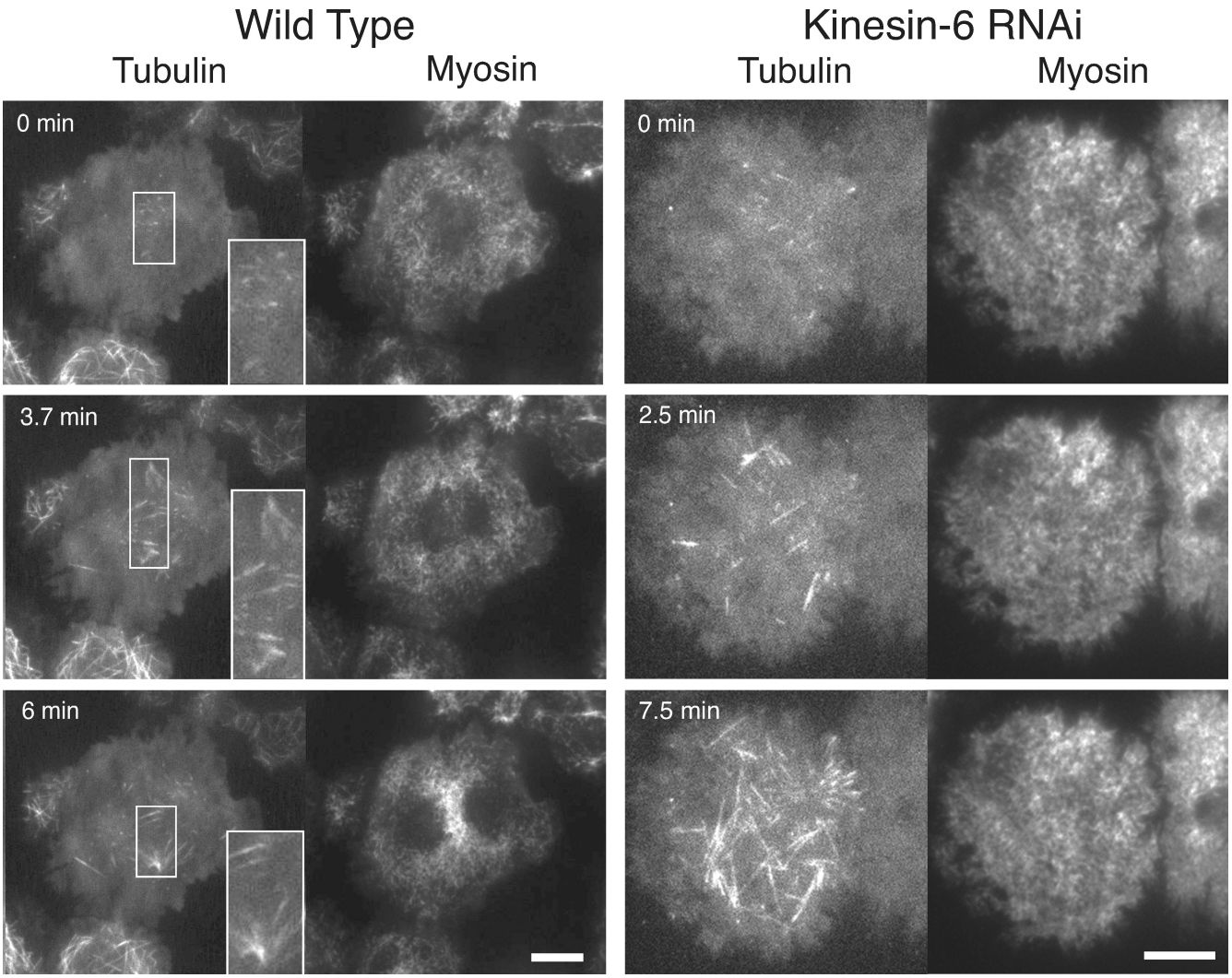

Figure 3. **Localization of microtubules and myosin at the cortex during anaphase in wild type and cells depleted of Kinesin-6 by RNAi.** mCherry-tubulin and myosin-GFP were imaged by dual-color TIRF microscopy. The insets in the wild-type cell show enlarged views of stable microtubule bundles that appear at the equatorial cortex within the TIRF illumination field. The interior, bipolar mitotic spindle is not visible by TIRF imaging but is aligned and extends perpendicular to the band of equatorial myosin accumulation (as in Fig. 1). Depletion of the Kinesin-6 motor by RNAi prevents both the accumulation of myosin-GFP at the equator and loss at the poles and reduces the number of equatorial microtubule bundles during anaphase. Although myosin does not accumulate at the equator, anaphase is noted by the increase in the number of microtubules that reach the cortex in the Kinesin-6 RNAi cells. Kinesin-6 RNAi cells also tend to have a more homogeneous pattern of myosin at the cortex during metaphase (compare 0 s time points). See Videos 2 (wild type) and 6 (Kinesin-6 RNAi). Bars, 10 µm.

around the position of the metaphase plate (Fig. 3 and Video 2). Individual microtubule tips appeared only transiently within the TIRF field (<30 s), which indicates that the microtubules that reached the cortex were unstable and underwent rapid catastrophe to a shrinking state. As cells entered anaphase, microtubule dynamics changed dramatically; more microtubules appeared at the cortex, a greater length of the microtubule became visible in the evanescent field, and the microtubules became more stable (many stable for several minutes). In most cells at anaphase onset, more microtubules initially appeared at the midzone cortex than the poles (Fig. 2). The greater microtubule density near the midzone at anaphase onset may be caused by augmin–γ-tubulin–mediated microtubule nucleation within the spindle, which is directed toward the chromosomes/midzone region (Mahoney et al., 2006; Goshima et al., 2008). Furthermore, S2 cells have relatively small centrosomal microtubule asters in comparison with those in sea urchin eggs (Foe and von Dassow. 2008) or early *C. elegans* embryos (Bringmann and Hyman, 2005), and also do not require functional centrosomes for forming spindles and segregating chromosomes (Mahoney et al., 2006). As anaphase progressed, microtubules continued to elongate and became more numerous throughout the cortex. These observations are consistent with prior work showing that microtubule-destabilizing proteins (e.g., depolymerizing Kinesin-13 motors) are activated during prometaphase/metaphase and then repressed in anaphase/interphase (Walczak and Heald, 2008). Of particular note, some microtubules near the equator became bundled at their tips, and these bundled microtubules were particularly stable (Fig. 3, insets). The region where the stable microtubules appeared was generally where myosin accumulated at the equatorial cortex. However, the correspondence was not precise, as myosin accumulated evenly in-between the microtubule bundles (e.g., 6 min in Fig. 3).

Different subsets of cortical microtubules have been implicated in specifying furrow location. Stable microtubules at the cortex have been suggested to induce furrow formation/contraction (Canman et al., 2003; Foe and von Dassow, 2008), but another study has proposed that a furrow forms when the asters move apart and create a local minimum of cortical microtubules at the midzone (Dechant and Glotzer, 2003). Studies also have implicated dynamic astral microtubules that extend toward the poles as agents that induce cortical polar relaxation (Foe and von Dassow, 2008; Murthy and Wadsworth, 2008). We explored how microtubule dynamics and distribution affect myosin localization by perturbing microtubules with RNAi (Fig. S3). To reduce the numbers of astral microtubules that reach the poles from the centrosomes, we inhibited centrosome-mediated microtubule nucleation by RNAi-mediated depletion of centrosomin (Cnn), a protein involved in recruiting the microtubule nucleator γ-tubulin to centrosomes (Megraw et al., 1999). Cnn-depleted S2 cells organize acentrosomal spindles that align and segregate chromosomes normally (Mahoney et al., 2006). By TIRF imaging, we found that myosin filaments disappear from the poles and appear at the midzone in a similar fashion to wild-type cells (Fig. S3 and Video 3). Thus, a radial microtubule aster emanating from the centrosome does not appear to be essential for myosin relocalization during anaphase in S2 cells (see Discussion). In addition, in untreated wild-type cells, we have observed situations where many astral microtubules contacted the cortex at one pole, but few microtubules were observed at the opposite pole (perhaps due to a tilt in the spindle axis). Despite this asymmetry, myosin disappeared at both poles to similar extents and at approximately similar times (Video 4). Thus, polar loss and equatorial accumulation of myosin appears to be relatively insensitive to the numbers of dynamic astral microtubules that contact the polar regions of the cell.

To further investigate the role of microtubule dynamics, we used RNAi to deplete Klp10A, a microtubule-destabilizing Kinesin-13 family member (Moores and Milligan, 2006). Unlike wild-type cells at metaphase, many microtubules in Klp10A-depleted cells reached the cell cortex and could be observed within the evanescent field for long periods of time (1–4 min; Fig. S3 and Video 3). Despite this premature appearance of stable microtubules at the cortex before anaphase, the redistribution of cortical myosin-GFP from metaphase to anaphase in Klp10A-depleted cells took place in a manner comparable to control cells (Fig. S3 and Video 3). Thus, although microtubules are clearly important for specifying the formation of the actomyosin contractile ring at the equator, this signaling mechanism is reasonably robust to changes in microtubule dynamics. A similar conclusion was reached by Strickland et al. (2005), who showed that furrow formation in sea urchin eggs required microtubule contact with the cortex but was minimally affected by changes in microtubule dynamics induced by drug treatments (hexylene glycol, taxol, and urethane).

Delivery of Kinesin-6 and Aurora B to the cortex

Kinesin-6 is required for cytokinesis in many eukaryotes, including *Drosophila* (called Pav in this organism; Glover et al., 2008). Kinesin-6 is thought to be important for activating RhoA (by delivering the Rho guanine nucleotide exchange factor Pebble/ECT2), and inactivating Rac (through its associated Rac GAP [RacGAP50C/CYK4]). In cells depleted of Kinesin-6 by RNAi, myosin-GFP was homogenously distributed in metaphase, and little change in its distribution occurred during anaphase; myosin neither accumulated at the equator nor became depleted at the poles (Fig. 3 and Video 6). However, the majority of Kinesin-6–depleted cells showed an increase in cortical myosin during anaphase (1.65 ± 0.66 increase; mean ± SD, n = 11 cells), which suggests that RhoA was activated but not in a localized region of the cell. Thus, Kinesin-6 is necessary for concentrating RhoA activity and myosin assembly at the equator but is also required for the loss of myosin filaments at the poles (see Discussion).

Previous GFP studies in *Drosophila* have shown that Pav localizes to the central spindle microtubules and the cell cortex at the cleavage furrow (Minestrini et al., 2003), and mammalian Kinesin-6 was found to localize to microtubule tips at the cortical midzone by immunofluorescence (Nishimura and Yonemura, 2006). However, high resolution, time-lapse imaging of Kinesin-6 at anaphase onset has not been performed. In metaphase S2 cells, we found that Kinesin-6–GFP particles (either single molecules or small aggregates) were distributed mostly uniformly over the cortex and generally appeared only transiently within the illumination field of TIRF (1–2 frames, 2 s each). However, upon entering anaphase, the diffuse cortical fluorescence of Kinesin-6–GFP diminished, and the protein appeared on the plus ends of microtubules and tracked along these tips as they grew toward the cortex (Fig. 4 and Video 5).

At the beginning of anaphase, Kinesin-6–GFP was found on many microtubule tips, many of which are likely to be single, growing microtubules. These Kinesin-6–microtubule tip complexes were visible at the cortex within the evanescent field for 0.5–4 min, but then Kinesin-6 was lost from the majority of microtubule tips, especially those positioned away from the midzone. We observed that Kinesin-6 was more stable and continued to accumulate when two microtubule tips came in close proximity (e.g., Fig. 4 B). Some of these microtubules intersect in a parallel manner (Fig. 4 B). However, Kinesin-6 tended to be the most concentrated and long-lived on the tips of intersecting presumably antiparallel microtubules located at the equatorial cortex. This behavior differed from the plus end–tracking protein EB1, which was located on the tips of growing microtubules but did not accumulate on tips of stable microtubules at the equator (Video 8). Interestingly, we also observed a diffuse "band" of Kinesin-6–GFP fluorescence across the midzone in many cells, which did not specifically colocalize with cortical microtubules (Fig. 4 A, 6 min). This observation suggests that the Kinesin-6 complex, in addition to binding to microtubules, docks to specific sites on the equatorial cortex.

The bright fluorescent Kinesin-6–GFP spots at the equator appeared to localize with bundled microtubules (Fig. 4). We therefore sought to examine whether Kinesin-6 is actively involved in the bundling and stability of these equatorial microtubules by examining the consequences of depleting Kinesin-6 (Pav) by RNAi (Fig. 3 and Video 6). Kinesin-6–depleted cells displayed none or few stable microtubule bundles at the equator (scored as bright foci of intersecting microtubules that persist for >2 min; one or two microtubule [MT] bundles scored per

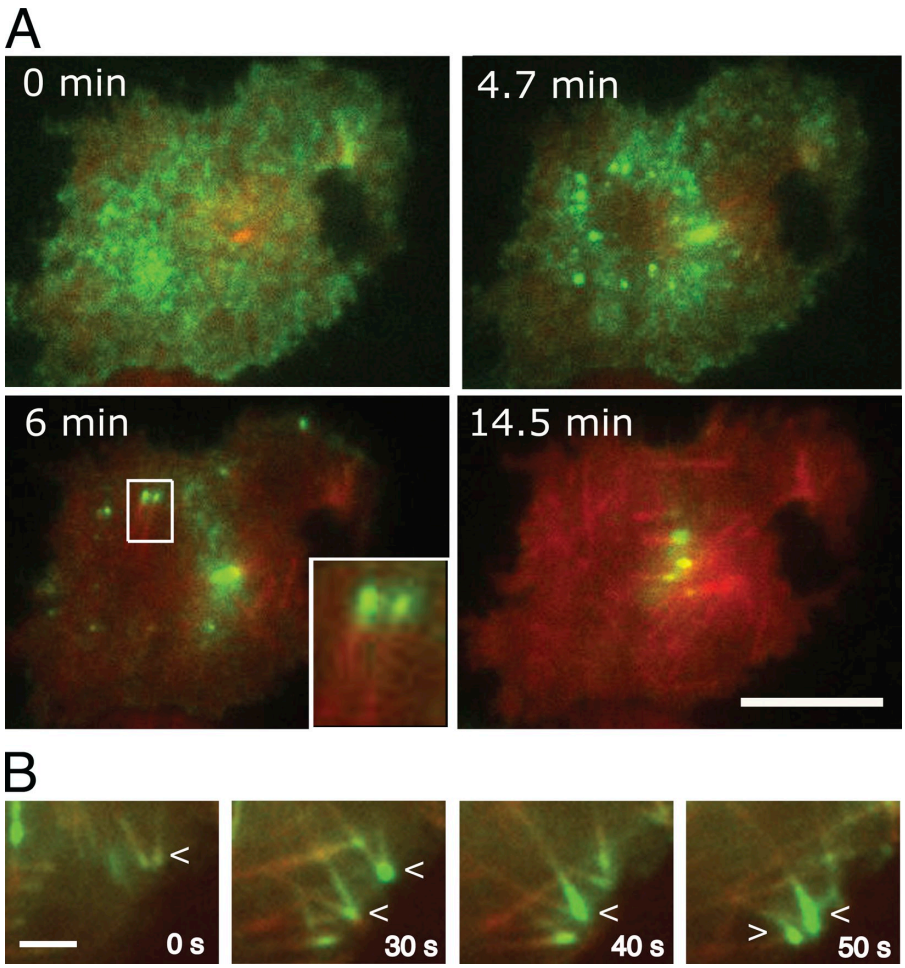

Figure 4. **Relocalization of Kinesin-6 to microtubule tips and the equatorial cortex during anaphase.** S2 cells coexpressing mCherry-tubulin (red) and Kinesin-6–GFP (green) were imaged by dual-color TIRF microscopy. (A) At the 0 min time point, the cell is in metaphase, and subsequent times are in anaphase. The inset at 6 min shows Kinesin-6–GFP colocalizing with the tips of microtubules. A diffuse equatorial band of Kinesin-6–GFP is also seen at this time point. At later time points, Kinesin-6–GFP is localized exclusively to the equator, which likely contains antiparallel microtubule bundles. Although the total Kinesin-6–GFP signal appears to diminish over time, the majority of the protein concentrates on the microtubules in the interior central spindle (Goshima and Vale, 2005), which is not visible or minimally visible by TIRF microscopy. See Video 5. Bar, 10 µm. (B) This time series from another cell shows microtubules that grow toward one another and increase levels of Kinesin-6–GFP when the microtubules come in close proximity (arrowheads), including in regions where the microtubules are not directly overlapping (40 s). Bar, 2 µm.

cell for Kinesin-6 RNAi cells versus two to four MT bundles per cell for wild-type cells [six cells each]). These results indicate that Kinesin-6 not only concentrates at equatorial MT bundles, but also appears to be a contributing factor for their stability.

In addition to its previously demonstrated localization on kinetochores in metaphase and the central spindle in anaphase (Fuller et al., 2008), we also found that Aurora B kinase (an activator of Kinesin-6; Guse et al., 2005) also localized on microtubules tips that grew toward the cortex at the beginning of anaphase (Fig. S4 and Video 7). Aurora B–GFP also localized to a diffuse band along the equatorial cortex. However, although depletion of Aurora B (which produces abnormal bipolar and monopolar spindles) perturbed the equatorial localization of Kinesin-6, it did not prevent the binding of Kinesin-6–GFP to microtubule tips during early anaphase (unpublished data).

In summary, our TIRF observations show that Kinesin-6–GFP is diffusely distributed throughout the cortex at metaphase, but relocalizes along with its activator Aurora B to microtubule tips that grow toward the cortex at the onset of anaphase. Within a couple of minutes, Kinesin-6 no longer associates with cortical microtubules further away from the equatorial zone and accumulates at the equator at the tips of microtubule bundles and along a diffuse equatorial band at or just beneath the cell membrane. The general pattern of Kinesin-6 localization at anaphase closely resembles the redistribution of myosin to the equator.

Localization of myosin and Kinesin-6 in monopolar spindles

A previous study by Canman et al. (2003) showed that cells with monopolar spindles (created by chemical inhibition of the Kinesin-5 motor) can form a cleavage furrow. This and a subsequent study by Hu et al. (2008) led to a model in which signals that specify cleavage furrow formation are released from chromosomes and travel along to the tips of stable microtubules. We examined the cortical localization of myosin-GFP in monopolar spindles that form after RNAi-mediated depletion of the *Drosophila* Kinesin-5 motor (Klp61F). Klp61F knockdown in S2 cells produces monopolar spindles where microtubules emanate from single centrosomal foci and chromosomes are found at the end of the microtubules. The majority of monopolar spindles are "asymmetric," with microtubules and chromosomes offset to one side, although a subset are "symmetric" (a more radial star burst pattern of microtubules and chromosomes; see gallery of mitotic spindles images for this gene knockdown at http://rnai.ucsf.edu; Goshima et al., 2007). We induced the Klp61F knockdown cells to enter anaphase (chromosomes moving from the periphery to the center) by simultaneously depleting the checkpoint protein, BubR1, which allows these monopolar cells to bypass the spindle assembly checkpoint.

After an asymmetric monopolar spindle entered anaphase, myosin-GFP accumulated at the cell periphery proximal to the

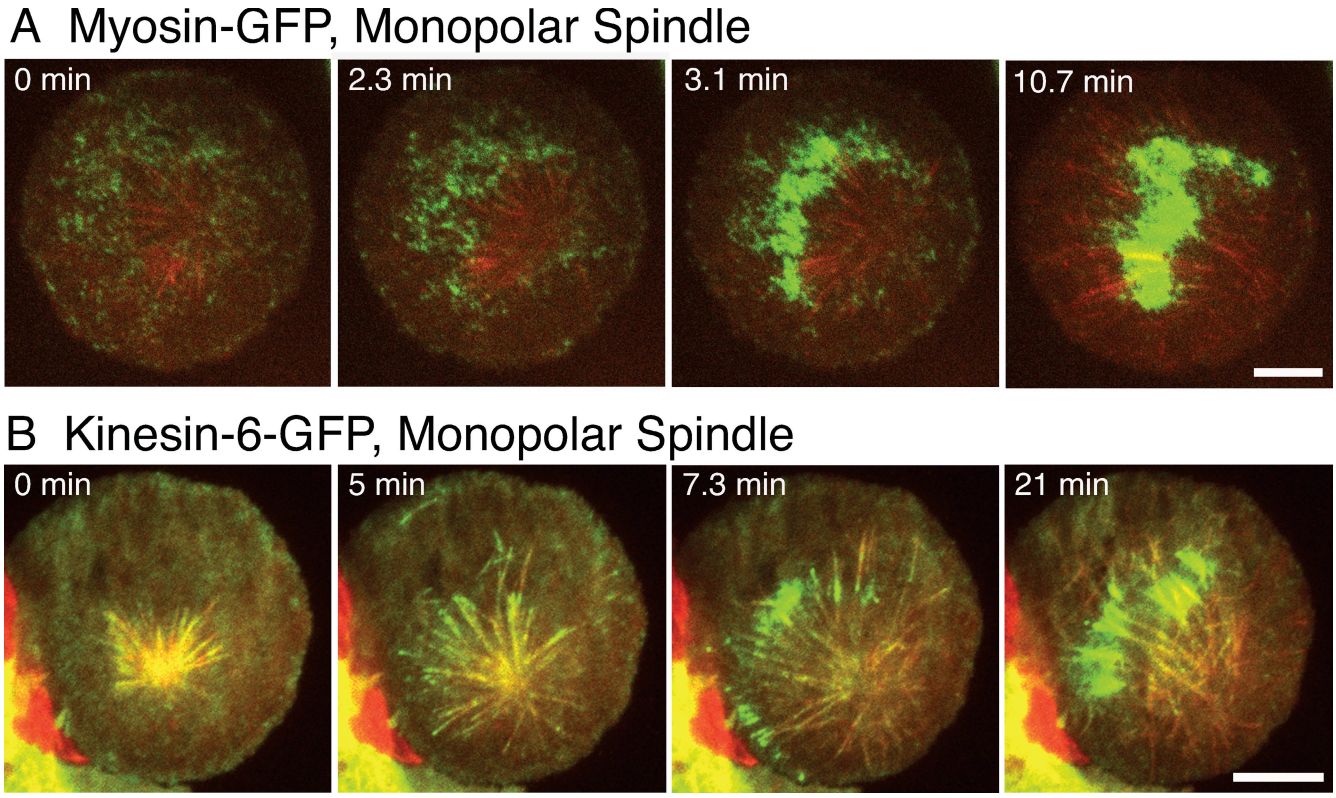

Figure 5. **Localization of myosin-GFP and Kinesin-6–GFP (Pav-GFP) in cells with monopolar spindles.** Monopolar spindles were induced by RNAi depletion of the Kinesin-5 motor (Klp61F in *Drosophila*); cells also were treated with dsRNA for BubR1, which causes these monopolar cells to bypass the spindle assembly checkpoint and proceed into anaphase. Cells were coexpressing mCherry-tubulin along with myosin-GFP (A) or Kinesin-6–GFP (B) and imaged by dual-color TIRF microscopy (note that different cells are shown in A and B). Both cells have asymmetric monopolar spindles, with most microtubules projecting toward one side of the cell. In A and B, myosin-GFP and Kinesin-6–GFP accumulate at the regions of microtubule plus ends during anaphase. See Videos 9 (myosin-GFP) and 5 (Kinesin-6–GFP). Bars, 10 µm.

greatest accumulation of microtubule plus ends (Fig. 5 A and Video 9). Although myosin was not imaged in earlier studies, this myosin localization is anticipated based upon on the location of the cleavage furrow in monopolar spindles (Canman et al., 2003). As myosin accumulated at the periphery, cortical myosin-GFP particles also disappeared from the more central regions of some cells (Fig. 5 A and Video 9). Thus, signals that induce the spatially segregated appearance and disappearance of myosin filaments operate in monopolar spindles. But in the case of monopolar spindles, myosin disappears from the central region of the cortex and accumulates at the surrounding peripheral cortex, whereas the opposite pattern occurs in bipolar spindles. However, these different patterns are consistent with the positioning of key components during anaphase in these two types of spindles; in both cases, myosin accumulates at microtubule plus ends and becomes depleted in regions of the centrosomes and chromosomes (which accumulate in the center in cells with monopolar spindles and move toward the poles in cells with elongating bipolar spindles).

After the initial and rapid accumulation of myosin-GFP at the periphery, we also observed a slower "self centering" that resulted in myosin accumulation toward the central region of the cortical footprint in some cells. This was particularly striking in "symmetric" monopolar spindles, which initially accumulated myosin evenly around the periphery but later would break symmetry and accumulate myosin closer to the middle of the cell (Fig. 6 and Video 10). A symmetry-breaking phenomenon also has been described for monopolar spindles in mammalian cells by Hu et al. (2008), which involves actomyosin, RhoA, and Aurora B kinase. However, in the case of Hu et al. (2008), the symmetry breaking involved the repositioning of cortical components to one side of the cell, rather than toward the middle as observed here for S2 cells. The repositioning of myosin toward the middle of the cortical footprint appears to involve a dynamic process of myosin appearing and disappearing at the surface, rather than by a centripetal flow of cortical myosin. For "asymmetric" monopolar spindles (most microtubules projecting to one side), the myosin mass that was initially asymmetrically positioned on one side of the cell also shifted somewhat toward the middle (Fig. 5 A).

We also examined Kinesin-6–GFP in cells with monopolar spindles (Fig. 5 B and Video 5). Kinesin-6–GFP tracked along the MT plus ends as microtubules elongated toward the cell periphery during anaphase, appearing as a radial starburst of fluorescent Kinesin-6–GFP spots. The Kinesin-6–MT complexes paused at the cortex, but then Kinesin-6–GFP dissociated from the majority of microtubule tips and eventually concentrated on a subset of cortical microtubules that were likely bundles (Fig. 5 B and Video 5; also note that a few microtubules were observed growing from the periphery to the center, so a subset of zones of concentrated Kinesin-6–GFP could involve antiparallel microtubules). Thus, the pattern of

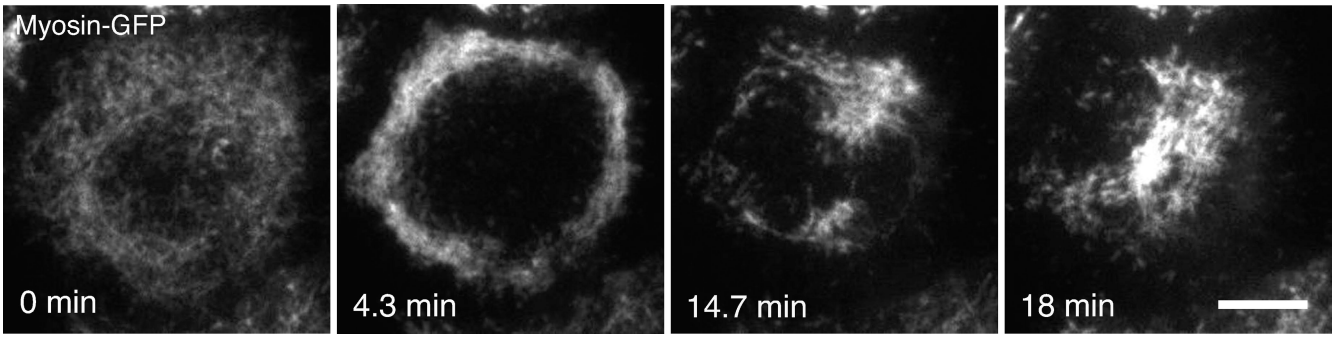

Figure 6. **Localization of myosin-GFP in a cell with a radially symmetrical monopolar spindle.** Monopolar anaphases were induced by RNAi depletions of the Kinesin-5 motor (Klp61F in *Drosophila*) and BubR1. This cell, imaged by TIRF microscopy, localizes myosin-GFP symmetrically at its periphery at early anaphase (4.3 min) but then redistributes the myosin toward the center of the cortical footprint more slowly (14.7 and 18 min). See Video 10. Bar, 10 µm.

Kinesin-6 distribution in monopolar spindles is generally similar to myosin localization.

Discussion

By imaging the cortex during anaphase using time-lapse TIRF microscopy, we have observed the dynamics of several key molecules involved in cytokinesis. Our observations show that myosin filaments are highly dynamic, rapidly appearing at the equatorial cortex and disappearing from the poles during the first minutes of anaphase. Our observations provide insight into how microtubules and Kinesin-6 might trigger the coordinated appearance and disappearance of myosin.

A positive signal for myosin filament accumulation at the cortex

The most prevalent hypothesis for the equatorial accumulation of myosin has been that the motor flows along the cortex from the pole to the equator during anaphase (Wang et al., 1994; DeBiasio et al., 1996; Yumura, 2001). However, by TIRF imaging in S2 cells, we did not observe cortical flow and instead found that myosin filaments abruptly appear at the midzone and disappear from the poles. While this work was in preparation, similar results were described by Zhou and Wang (2008) in HeLa cells, Yumura et al. (2008) in *D. discoideum*, and Foe and von Dassow (2008) in sea urchin eggs. Using myosin mutations that stabilize filament formation, Yumura et al. (2008) also observed cortical flow of myosin toward the equator, revealing that cortical flow may assist the equatorial concentration mechanism in some cell types. However, the dominant mechanisms for myosin appearance at the equator most likely reflect local Rho activation followed by downstream de novo myosin filament assembly and actin engagement (resulting at least in part from regulatory light chain phosphorylation; Dean and Spudich, 2006; Uehara et al., 2008), the association of myosin filaments with parallel actin filaments created by formins (Dean et al., 2005), and the interactions of myosin with membrane-associated scaffold proteins such as septins (Joo et al., 2007) and anillin (Straight et al., 2005; Piekny and Glotzer, 2008).

Recent work has suggested that stable microtubules at the equator play an important role in establishing the furrow (Canman et al., 2003; Shannon et al., 2005; Foe and von Dassow, 2008; Murthy and Wadsworth, 2008). We also observed stable microtubules appearing at anaphase onset, but very few stable microtubules are present within the TIRF illumination field during the time when myosin filaments appear throughout the equator. Thus, relatively few cortical microtubules are sufficient to convey a signal that results in massive cortical myosin accumulation. Our work and that of many others (Adams et al., 1998; Mishima et al., 2002; Goshima and Vale, 2003; Minestrini et al., 2003; Yüce et al., 2005; Odell and Foe, 2008) suggests that the microtubule signal may arise from Kinesin-6 in complex with Rho family regulatory proteins. The Kinesin-6–RacGAP complex also has potent microtubule-bundling activity (Mishima et al., 2002), and our results also show that this Kinesin is a key agent involved in bundling microtubules at the cortex.

A critical remaining question is how Kinesin-6 selects the subset of microtubules at the equator, and not astral microtubules elsewhere on the cortex, to stimulate Rho and suppress Rac (Canman et al., 2008). Odell and Foe (2008) proposed and computationally tested a model in which Kinesin-6 binds to and moves along all microtubules at anaphase. Dynamic microtubules (e.g., ones directed to the poles) were proposed to disassemble before or shortly after reaching the cortex, and thus do not effectively deliver the Kinesin-6–Rho regulator complex. In contrast, stable microtubules at the equator can act as more permanent tracks for the continuous and efficient cortical delivery of the Kinesin-6–Rho regulatory complex. Interestingly, their computational model also required that Kinesin-6 should stall and accumulate at the ends of the equatorial microtubules, rather than running off of the tracks when the motor reaches the end. Our observations confirm aspects of the Odell and Foe (2008) model. At anaphase, we observed Kinesin-6 accumulating on microtubule ends as they grow toward the cortex, which is a critical part of their model (this is also consistent with immunofluorescence images of MKLP1 in HeLa cells; Nishimura and Yonemura, 2006). We also see an overall reduction in cortical Kinesin-6 at anaphase onset (Fig. 4 A), which is again consistent with the idea of Odell and Foe (2008) that the microtubule network acts as a "sink" that binds and depletes Kinesin-6 from the cortex. The mechanism of microtubule tip localization of Kinesin-6, however, is unclear from our present observations. We have not been able to observe Kinesin-6–GFP molecules moving unidirectionally along microtubules, so we cannot ascertain whether Kinesin-6 reaches the ends of

microtubules through its motor activity (Mishima et al., 2004) or whether it tracks along the growing end like a +TIP protein (Lansbergen and Akhmanova, 2006). However, Kinesin-6 might have a higher affinity for microtubule plus ends, as overexpressed Kinesin-6–GFP localizes to, bundles, and stabilizes microtubule plus ends in interphase S2 cells (unpublished data). Such plus end binding and bundling may be intrinsic properties of the Kinesin-6 motor complex, and cyclin-dependent kinase phosphorylation may be required to repress these activities during prometaphase/metaphase (Mishima et al., 2004; Goshima and Vale, 2005).

In addition to the interaction of Kinesin-6 with microtubules, we also observed an association of Kinesin-6 with the cortex in regions that are devoid of microtubules, which has not been observed in other studies. In metaphase, Kinesin-6 is distributed throughout the cortex, but at anaphase, this broad cortical localization is lost, and Kinesin-6 appears later as a stripe across the equator, similar to what has been described for Rho and the RhoGEF Pebble (Nishimura and Yonemura, 2006) and to what we find for the actin-nucleating protein Diaphanous (Fig. S1). This localization suggests that the Kinesin-6 complex interacts with a binding partner in the membrane or with particular proteins in the cortical actin network. The RacGAP has been shown to bind to Anillin, which could serve to localize the Kinesin-6–RacGAP complex directly to the nascent actomyosin ring (Gregory et al., 2008). The broad cortical association of Kinesin-6 may explain why myosin accumulates evenly throughout the equatorial cortex and not just in the vicinity of the few cortical microtubules at the equator (Fig. 3).

Our observations also suggest additional levels of complexity and likely regulation of Kinesin-6. Odell and Foe (2008) proposed that Kinesin-6 reaches the equatorial cortex by traveling on stable microtubules; in other regions of the cell, Kinesin-6 would rarely reach the cortex because these microtubules undergo catastrophe and depolymerize before they could deposit their cargo. However, we find that Kinesin-6 reaches the cortex on the tips of growing microtubules in many locations at the very earliest stage of anaphase. Later, Kinesin-6 dissociates from the microtubule plus ends that are more distant from the equator, whereas the equatorial microtubules gain more Kinesin-6 and become more bundled. In this manner, the distribution of cortical Kinesin-6 sharpens over the first couple of minutes of anaphase. A similar general type of phenomenon occurs in monopolar spindles, where Kinesin-6–GFP reaches the cortex on many microtubules that extend radially toward the periphery but later concentrates on a subset of microtubules.

How Kinesin-6 refines its cortical localization in bipolar and monopolar spindles is not known, but several mechanisms are possible. One possibility is that activation of Rho feeds back to enhance the localization of Kinesin-6 on microtubules and the cortical membrane/actin, which in turn would result in a further enhancement of Rho activity. Microtubule bundling, through Kinesin-6 and other cross-linking proteins such a PRC1/Feo, also might have the effect of enhancing Kinesin-6 localization by reducing its dissociation rate. Our observations suggest that Kinesin-6 might bundle both parallel and antiparallel microtubules (Fig. 4). However, if Kinesin-6 has a lower dissociation rate from antiparallel microtubules, this might enhance its equatorial localization in bipolar spindles over time (because microtubules from the two poles tend to overlap in this region). In bipolar spindles, the microtubule bundles in the interior central spindle also may aid in refining the position of the contractile ring by providing a large reservoir of Kinesin-6 and Aurora B kinase that can reach the equatorial astral microtubules by diffusion. Consistent with this idea, a gradient of Aurora B activity arising from the central spindle has been recently measured using Förster resonance energy transfer microscopy (Fuller et al., 2008). Such a general model could explain the independent but synergistic roles of astral and central spindle microtubules in furrow formation (Bringmann and Hyman, 2005) and our observed concentration of Kinesin-6 at the equator over time. However, the central spindle is not absolutely essential for cytokinesis (Verbrugghe and White, 2004), so it may serve to make the process more robust. Given the importance of localizing Kinesin-6, it would not be surprising if several redundant mechanisms operate to refine its localization to the equatorial cortex.

The signal for myosin disassembly at the poles

The mechanism responsible for the disassembly of myosin at the poles (polar relaxation) is much less well understood than the one that leads to myosin accumulation at the equator. Our RNAi depletion of Kinesin-6 in S2 cells suggests that the polar loss and the equatorial accumulation of myosin are coupled, and that both require this motor protein–Rho regulatory complex (Fig. 3). In their computational model, Odell and Foe (2008) proposed that Kinesin-6 is depleted from the polar cortex at anaphase as a result of its binding and sequestration on microtubules, thereby resulting in a reduction in cortical RhoA activity at the poles and consequential downstream loss of myosin filaments. Our experimental results showing that the polar loss of myosin requires Kinesin-6 supports their hypothesis. Thus, the loss of myosin filaments at the cortical poles, at least in part, appears to be caused by the removal/distribution of Rho activators.

In addition to removal of an activator (Kinesin-6 complex), it also has been suggested that highly dynamic microtubules extending from centrosomal asters might carry inhibitory signals to the polar cortex that disassemble myosin (Foe and von Dassow, 2008; Murthy and Wadsworth, 2008). However, we find that perturbations of (Fig. S3) or asymmetries in the astral microtubule array (Video 4) have minimal effects on the loss of myosin from the polar regions of S2 cells during anaphase. Nevertheless, some of our observations suggest that a signal may arise from the spindle that promotes myosin filament disassembly or the cortical dissociation of Rho activators. Specifically, we find that the center of the cortical footprint of metaphase S2 cells is often lacking in cortical myosin filaments ("donut-shaped hole" in Figs. 1 and 2). This "hole" might arise from bringing the mitotic spindle close to the cortex as a consequence of flattening the S2 cell on Con A surfaces, but nevertheless, it suggests that some inhibitory signal might diffuse from the mitotic spindle. During anaphase, the loss of myosin from the cortex also sweeps from more central to peripheral (polar) regions of the cortex along the line of spindle elongation and chromosome movement (Videos 1–3). A loss of cortical myosin filaments occurs in monopolar spindles, but in this case, occurs at the center of the cortical footprint where

centrosomes and chromosomes accumulate (Fig. 6 and Video 10). In S2 cells (which may differ from echinoderm eggs with regard to aspects of their mechanism for cytokinesis), these observations suggest that the disassembly of cortical myosin at anaphase may be facilitated by a diffusible signal emanating from chromosomes or spindle poles, rather than dynamic astral microtubules that touch the cortex. However, the existence of the signal is still speculative and its exact nature and how it might be coordinated with Kinesin-6 remains unknown.

In summary, the rapid myosin recruitment to the furrow and its depletion from the poles suggests that the formation of myosin filaments and their association with the cortex are dynamic processes that are responsive to RhoA activity. RhoA activity is likely controlled by the Kinesin-6 motor (perhaps in conjunction with its activating kinase Aurora B), which serves as a readout of spindle geometry. Several mechanisms are likely involved in sharpening Kinesin-6 localization and RhoA activation to the midzone in bipolar spindles and perhaps in causing the slower symmetry breaking and centering in monopolar spindles. Such mechanisms could involve local feedback circuits at the cortex, microtubule bundling, and diffusible gradients of Kinesin-6/Aurora B arising from the microtubule-dense central spindle. The transfer of Kinesin-6 from the cortex to microtubules at anaphase, perhaps in conjunction with a signal emanating from the elongating spindle, also promotes the loss of myosin from the poles and thereby sharpens myosin localization at the equator. Understanding the details and interactions of these multiple pathways using experimental and computational tools constitutes an important, upcoming challenge. In addition, different cells/organisms are likely to vary in how they use these redundant mechanisms, as we now know is true for the formation of the mitotic spindle (Walczak and Heald, 2008).

Materials and methods

Constructs, cell lines, and RNAi

Drosophila S2 cells were grown and RNAi was performed as described previously (Rogers et al., 2002). A construct using the endogenous promoter to express GFP fused to the regulatory light chain of myosin II (referred to as myosin-GFP in this paper) was described by Rogers et al. (2004). The GFP variant mCherry was fused to the N terminus of α-tubulin and expressed from the Act5c promoter, as first described and used in Goshima et al. (2007). Kinesin-6–GFP (Goshima and Vale, 2005) was expressed from a regulated metallothionein promoter (pMT) by the addition of 20–100 μM $CuSO_4$ overnight. GFP was fused to the C terminus of the Diaphanous gene (cDNA generously provided by M. Peifer, University of North Carolina, Chapel Hill, NC) using the using the Gateway system (Invitrogen). The Aurora B–GFP construct was obtained from G. Hickson (University of California, San Francisco, San Francisco, CA). Actin-GFP was first described in Rogers et al. (2003). EB1-GFP was described in Rogers et al. (2002). Stable cell lines (used for all experiments) were made by transfection with Effectene (QIAGEN) according to the manufacturer's instructions and then selected with hygromycin for ∼3 wk. The cell line stably expressing EB1-GFP and mCherry–α-tubulin was created by S. Goodwin (University of California, San Francisco). The Pav-GFP–transfected cells were FACS sorted and used shortly after selection, as the percentage of cells expressing both Pav-GFP and mCherry-tubulin cells decreased considerably over time. RNAi was performed as described previously, with essentially 1 μg double-stranded RNA (dsRNA) added per well in a 96-well plate (Rogers et al., 2002). RNAi treatment for Pav, Rho1, Cnn, and Klp10A was performed for 4–5 d, whereas double RNAi for Klp61F and BubR1 (to create monopolar spindles that progress into anaphase) was performed for 3 d. To control for any nonspecific RNAi effects, a control RNAi treatment was performed (5 d) with dsRNA to a 400–base pair region of the pBlueScript vector. Sequence information for the dsRNAs can be found at http://rnai.ucsf.edu/ (V2 library).

Microscopy and analysis

S2 cells were plated on MatTek dishes with No. 1.5 glass coverslip bottoms that were coated with Con A (0.5 mg/ml Con A [Sigma-Aldrich] air dried onto the coverslip) and allowed to spread for 1–3 h before imaging (Rogers et al., 2002). Total internal reflection microscopy was performed using a microscope (Perfect-focus TE2000; Nikon) with a 100×, 1.45 NA objective (Nikon) and illumination from either a 488-nm argon laser (100 mW) or a 491-nm solid-state laser (100 mW) and a 561-nm solid-state laser (50 mW). For dual-color TIRF microscopy, we used a triple-pass dichroic filter (z491/561/633rpc) and changed the emission filter (ET525/50 or ET595/50; both from Chroma Technology Corp.) with a filter wheel placed before the camera. In some cases, an excitation notch filter was used in the filter cube (NF01-405/488/561/635; Semrock, Inc.). Images were typically captured every 2–3 s with a 50–200-ms exposure with an EM charge-coupled device camera (iXon; Andor Technology). The microscope was controlled and images were acquired using open source MicroManager software (http://www.micro-manager.org). Images were cropped and contrast adjustments were made in Photoshop (Adobe).

We first searched for doubly transfected (mCherry and GFP fusions) metaphase cells by visualizing their spindle with mCherry-tubulin using epifluorescence, and then switched to TIRF microscopy. (Because of the difficulty in identifying mitotic cells, we were unable to study cells transfected with Pav-GFP and myosin-mCherry.) Cells that did not enter anaphase within 30 min or with high levels of fluorescence from overexpressed proteins were excluded from analysis. Results are representative of six or more cells. Image analysis was performed using ImageJ software (http://rsbweb.nih.gov/ij/).

Online supplemental material

Fig. S1 shows the distribution of actin-GFP and diaphanous-GFP during anaphase. Fig. S2 shows the time course of disappearance of an individual myosin filament. Fig. S3 and Video 3 show that myosin-GFP relocalization during anaphase proceeds normally after RNAi knockdown of centrosomin (which blocks microtubule nucleation at centrosomes) and Klp10A (which increases the number of stable microtubules at the cortex). Video 6 shows that myosin-GFP localization to the midzone and loss from the poles does not occur after RNAi Kinesin-6; microtubules tend to be more homogeneous throughout the cortex and less bundled. Fig. S4 and Video 7 show Aurora B–GFP on the tips of microtubules as they grow toward the cortex during early anaphase. Video 8 shows the behavior of EB1-GFP at the cortex during anaphase, and Video 4 shows a cell where microtubule asters from one centrosome reach the cortex but do not on the other side. Videos 1, 2, 5, 9, and 10 present dynamic data of the cells shown in Figs. 1; 3; 5, b and a; and 6, respectively. Online supplemental material is available at http://www.jcb.org/cgi/content/full/jcb.200902083/DC1.

We are grateful to several students from the Woods Hole Physiology Course who contributed to this study: Monica Bettencourt-Dias, Michela Zucculo, Sarah Gierke, and Lanying Zeng. We thank Gilles Hickson for providing the Aurora B–GFP construct and M. Peifer for the Diaphanous cDNA. We thank Steve Ross and Nikon, Inc., for the generous loan of Nikon microscopes at the Woods Hole Physiology Course and for post-course research.

This work was supported by a National Institutes of Health grant NIH 38499 to R.D. Vale.

This paper is dedicated to the memory of Barbara Dell.

Submitted: 17 February 2009
Accepted: 27 July 2009

References

Adams, R.R., A.A. Tavares, A. Salzberg, H.J. Bellen, and D.M. Glover. 1998. pavarotti encodes a kinesin-like protein required to organize the central spindle and contractile ring for cytokinesis. *Genes Dev.* 12:1483–1494.

Bement, W.M., H.A. Benink, and G. von Dassow. 2005. A microtubule-dependent zone of active RhoA during cleavage plane specification. *J. Cell Biol.* 170:91–101.

Bringmann, H., and A.A. Hyman. 2005. A cytokinesis furrow is positioned by two consecutive signals. *Nature.* 436:731–734.

Canman, J.C., D.B. Hoffman, and E.D. Salmon. 2000. The role of pre- and post-anaphase microtubules in the cytokinesis phase of the cell cycle. *Curr. Biol.* 10:611–614.

Canman, J.C., L.A. Cameron, P.S. Maddox, A. Straight, J.S. Tirnauer, T.J. Mitchison, G. Fang, T.M. Kapoor, and E.D. Salmon. 2003. Determining the position of the cell division plane. *Nature.* 424:1074–1078.

Canman, J.C., L. Lewellyn, K. Laband, S.J. Smerdon, A. Desai, B. Bowerman, and K. Oegema. 2008. Inhibition of Rac by the GAP activity of centralspindlin is essential for cytokinesis. *Science.* 322:1543–1546.

D'Avino, P.P., M.S. Savoian, and D.M. Glover. 2005. Cleavage furrow formation and ingression during animal cytokinesis: a microtubule legacy. *J. Cell Sci.* 118:1549–1558.

Dean, S.O., and J.A. Spudich. 2006. Rho kinase's role in myosin recruitment to the equatorial cortex of mitotic *Drosophila* S2 cells is for myosin regulatory light chain phosphorylation. *PLoS One.* 1:e131.

Dean, S.O., S.L. Rogers, N. Stuurman, R.D. Vale, and J.A. Spudich. 2005. Distinct pathways control recruitment and maintenance of myosin II at the cleavage furrow during cytokinesis. *Proc. Natl. Acad. Sci. USA.* 102:13473–13478.

DeBiasio, R.L., G.M. LaRocca, P.L. Post, and D.L. Taylor. 1996. Myosin II transport, organization, and phosphorylation: evidence for cortical flow/solation-contraction coupling during cytokinesis and cell locomotion. *Mol. Biol. Cell.* 7:1259–1282.

Dechant, R., and M. Glotzer. 2003. Centrosome separation and central spindle assembly act in redundant pathways that regulate microtubule density and trigger cleavage furrow formation. *Dev. Cell.* 4:333–344.

Eggert, U.S., T.J. Mitchison, and C.M. Field. 2006. Animal cytokinesis: from parts list to mechanisms. *Annu. Rev. Biochem.* 75:543–566.

Foe, V.E., and G. von Dassow. 2008. Stable and dynamic microtubules coordinately shape the myosin activation zone during cytokinetic furrow formation. *J. Cell Biol.* 183:457–470.

Fuller, B.G., M.A. Lampson, E.A. Foley, S. Rosasco-Nitcher, K.V. Le, P. Tobelmann, D.L. Brautigan, P.T. Stukenberg, and T.M. Kapoor. 2008. Midzone activation of aurora B in anaphase produces an intracellular phosphorylation gradient. *Nature.* 453:1132–1136.

Glotzer, M. 2009. The 3Ms of central spindle assembly: microtubules, motors and MAPs. *Nat. Rev. Mol. Cell Biol.* 10:9–20.

Glover, D.M., L. Capalbo, P.P. D'Avino, M.K. Gatt, M.S. Savoian, and T. Takeda. 2008. Girds 'n' cleeks o' cytokinesis: microtubule sticks and contractile hoops in cell division. *Biochem. Soc. Trans.* 36:400–404.

Goshima, G., and R.D. Vale. 2003. The roles of microtubule-based motor proteins in mitosis: comprehensive RNAi analysis in the *Drosophila* S2 cell line. *J. Cell Biol.* 162:1003–1016.

Goshima, G., and R.D. Vale. 2005. Cell cycle-dependent dynamics and regulation of mitotic kinesins in *Drosophila* S2 cells. *Mol. Biol. Cell.* 16:3896–3907.

Goshima, G., R. Wollman, S.S. Goodwin, N. Zhang, J.M. Scholey, R.D. Vale, and N. Stuurman. 2007. Genes required for mitotic spindle assembly in *Drosophila* S2 cells. *Science.* 316:417–421.

Goshima, G., M. Mayer, N. Zhang, N. Stuurman, and R.D. Vale. 2008. Augmin: a protein complex required for centrosome-independent microtubule generation within the spindle. *J. Cell Biol.* 181:421–429.

Gregory, S.L., S. Ebrahimi, J. Milverton, W.M. Jones, A. Bejsovec, and R. Saint. 2008. Cell division requires a direct link between microtubule-bound RacGAP and Anillin in the contractile ring. *Curr. Biol.* 18:25–29.

Guse, A., M. Mishima, and M. Glotzer. 2005. Phosphorylation of ZEN-4/MKLP1 by aurora B regulates completion of cytokinesis. *Curr. Biol.* 15:778–786.

Hu, C.K., M. Coughlin, C.M. Field, and T.J. Mitchison. 2008. Cell polarization during monopolar cytokinesis. *J. Cell Biol.* 181:195–202.

Inoue, Y.H., M.S. Savoian, T. Suzuki, E. Máthé, M.T. Yamamoto, and D.M. Glover. 2004. Mutations in orbit/mast reveal that the central spindle is comprised of two microtubule populations, those that initiate cleavage and those that propagate furrow ingression. *J. Cell Biol.* 166:49–60.

Joo, E., M.C. Surka, and W.S. Trimble. 2007. Mammalian SEPT2 is required for scaffolding nonmuscle myosin II and its kinases. *Dev. Cell.* 13:677–690.

Kamijo, K., N. Ohara, M. Abe, T. Uchimura, H. Hosoya, J.S. Lee, and T. Miki. 2006. Dissecting the role of Rho-mediated signaling in contractile ring formation. *Mol. Biol. Cell.* 17:43–55.

Lansbergen, G., and A. Akhmanova. 2006. Microtubule plus end: a hub of cellular activities. *Traffic.* 7:499–507.

Mahoney, N.M., G. Goshima, A.D. Douglass, and R.D. Vale. 2006. Making microtubules and mitotic spindles in cells without functional centrosomes. *Curr. Biol.* 16:564–569.

Megraw, T.L., K. Li, L.R. Kao, and T.C. Kaufman. 1999. The centrosomin protein is required for centrosome assembly and function during cleavage in *Drosophila*. *Development.* 126:2829–2839.

Miller, A.L., and W.M. Bement. 2009. Regulation of cytokinesis by Rho GTPase flux. *Nat. Cell Biol.* 11:71–77.

Miller, A.L., G. von Dassow, and W.M. Bement. 2008. Control of the cytokinetic apparatus by flux of the Rho GTPases. *Biochem. Soc. Trans.* 36:378–380.

Minestrini, G., A.S. Harley, and D.M. Glover. 2003. Localization of Pavarotti-KLP in living *Drosophila* embryos suggests roles in reorganizing the cortical cytoskeleton during the mitotic cycle. *Mol. Biol. Cell.* 14:4028–4038.

Mishima, M., S. Kaitna, and M. Glotzer. 2002. Central spindle assembly and cytokinesis require a kinesin-like protein/RhoGAP complex with microtubule bundling activity. *Dev. Cell.* 2:41–54.

Mishima, M., V. Pavicic, U. Grüneberg, E.A. Nigg, and M. Glotzer. 2004. Cell cycle regulation of central spindle assembly. *Nature.* 430:908–913.

Moores, C.A., and R.A. Milligan. 2006. Lucky 13-microtubule depolymerisation by kinesin-13 motors. *J. Cell Sci.* 119:3905–3913.

Murthy, K., and P. Wadsworth. 2008. Dual role for microtubules in regulating cortical contractility during cytokinesis. *J. Cell Sci.* 121:2350–2359.

Nishimura, Y., and S. Yonemura. 2006. Centralspindlin regulates ECT2 and RhoA accumulation at the equatorial cortex during cytokinesis. *J. Cell Sci.* 119:104–114.

Odell, G.M., and V.E. Foe. 2008. An agent-based model contrasts opposite effects of dynamic and stable microtubules on cleavage furrow positioning. *J. Cell Biol.* 183:471–483.

Piekny, A.J., and M. Glotzer. 2008. Anillin is a scaffold protein that links RhoA, actin, and myosin during cytokinesis. *Curr. Biol.* 18:30–36.

Piekny, A., M. Werner, and M. Glotzer. 2005. Cytokinesis: welcome to the Rho zone. *Trends Cell Biol.* 15:651–658.

Rappaport, R. 1971. Cytokinesis in animal cells. *Int. Rev. Cytol.* 31:169–213.

Rogers, S.L., G.C. Rogers, D.J. Sharp, and R.D. Vale. 2002. *Drosophila* EB1 is important for proper assembly, dynamics, and positioning of the mitotic spindle. *J. Cell Biol.* 158:873–884.

Rogers, S.L., U. Wiedemann, N. Stuurman, and R.D. Vale. 2003. Molecular requirements for actin-based lamella formation in *Drosophila* S2 cells. *J. Cell Biol.* 162:1079–1088.

Rogers, S.L., U. Wiedemann, U. Häcker, C. Turck, and R.D. Vale. 2004. *Drosophila* RhoGEF2 associates with microtubule plus ends in an EB1-dependent manner. *Curr. Biol.* 14:1827–1833.

Shannon, K.B., J.C. Canman, C. Ben Moree, J.S. Tirnauer, and E.D. Salmon. 2005. Taxol-stabilized microtubules can position the cytokinetic furrow in mammalian cells. *Mol. Biol. Cell.* 16:4423–4436.

Somers, W.G., and R. Saint. 2003. A RhoGEF and Rho family GTPase-activating protein complex links the contractile ring to cortical microtubules at the onset of cytokinesis. *Dev. Cell.* 4:29–39.

Straight, A.F., C.M. Field, and T.J. Mitchison. 2005. Anillin binds nonmuscle myosin II and regulates the contractile ring. *Mol. Biol. Cell.* 16:193–201.

Strickland, L.I., E.J. Donnelly, and D.R. Burgess. 2005. Induction of cytokinesis is independent of precisely regulated microtubule dynamics. *Mol. Biol. Cell.* 16:4485–4494.

Uehara, R., H. Hosoya, and I. Mabuchi. 2008. In vivo phosphorylation of regulatory light chain of myosin II in sea urchin eggs and its role in controlling myosin localization and function during cytokinesis. *Cell Motil. Cytoskeleton.* 65:100–115.

Verbrugghe, K.J., and J.G. White. 2004. SPD-1 is required for the formation of the spindle midzone but is not essential for the completion of cytokinesis in *C. elegans* embryos. *Curr. Biol.* 14:1755–1760.

Walczak, C.E., and R. Heald. 2008. Mechanisms of mitotic spindle assembly and function. *Int. Rev. Cytol.* 265:111–158.

Wang, Y.L., J.D. Silverman, and L.G. Cao. 1994. Single particle tracking of surface receptor movement during cell division. *J. Cell Biol.* 127:963–971.

Watanabe, S., Y. Ando, S. Yasuda, H. Hosoya, N. Watanabe, T. Ishizaki, and S. Narumiya. 2008. mDia2 induces the actin scaffold for the contractile ring and stabilizes its position during cytokinesis in NIH 3T3 cells. *Mol. Biol. Cell.* 19:2328–2338.

Yoshizaki, H., Y. Ohba, K. Kurokawa, R.E. Itoh, T. Nakamura, N. Mochizuki, K. Nagashima, and M. Matsuda. 2003. Activity of Rho-family GTPases during cell division as visualized with FRET-based probes. *J. Cell Biol.* 162:223–232.

Yüce, O., A. Piekny, and M. Glotzer. 2005. An ECT2-centralspindlin complex regulates the localization and function of RhoA. *J. Cell Biol.* 170:571–582.

Yumura, S. 2001. Myosin II dynamics and cortical flow during contractile ring formation in *Dictyostelium* cells. *J. Cell Biol.* 154:137–146.

Yumura, S., M. Ueda, Y. Sako, T. Kitanishi-Yumura, and T. Yanagida. 2008. Multiple mechanisms for accumulation of myosin II filaments at the equator during cytokinesis. *Traffic.* 9:2089–2099.

Zhou, M., and Y.L. Wang. 2008. Distinct pathways for the early recruitment of myosin II and actin to the cytokinetic furrow. *Mol. Biol. Cell.* 19:318–326.

Published

Vale et al., http://www.jcb.org/cgi/content/full/jcb.200902083/DC1

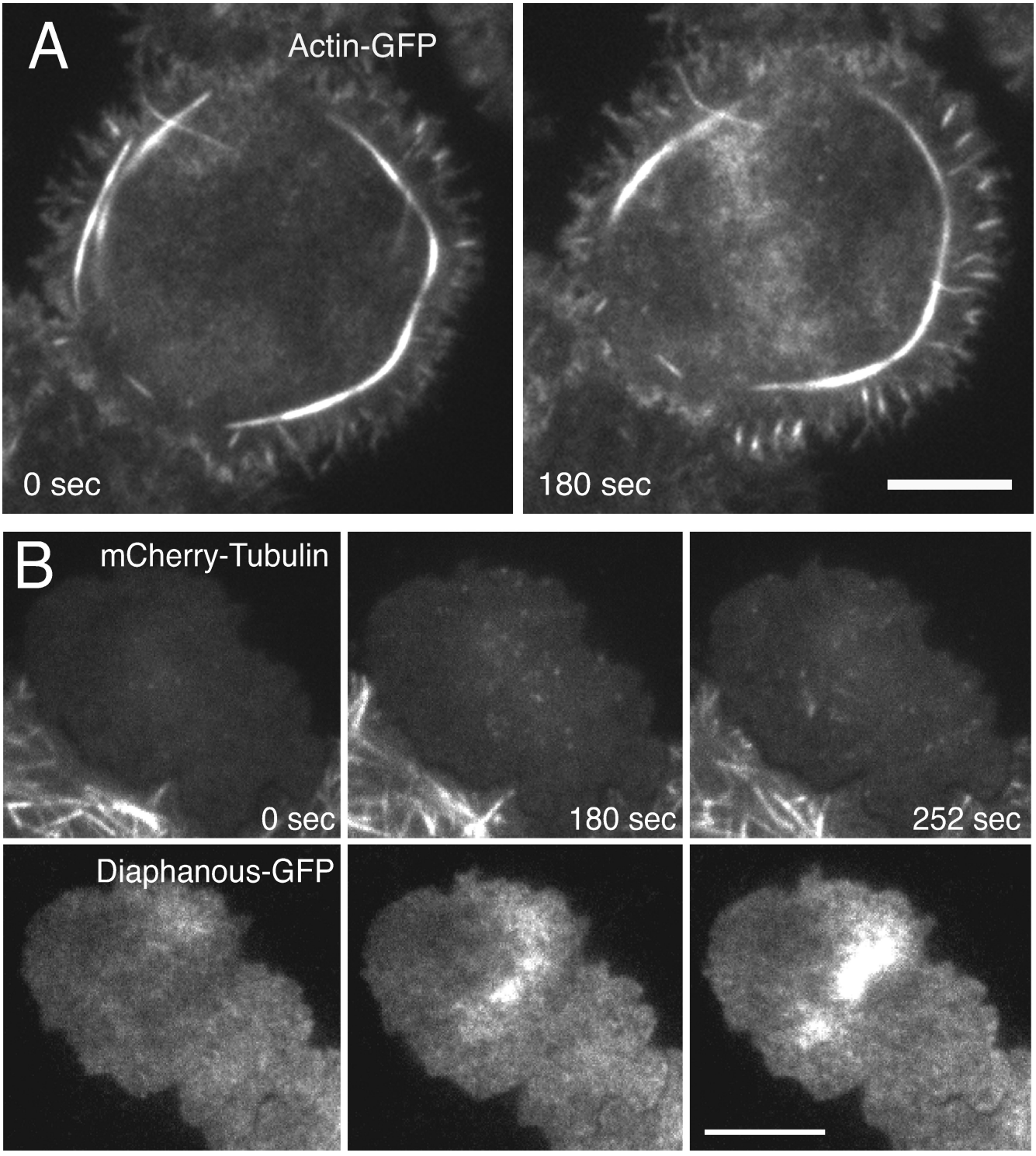

Figure S1. **Actin and the actin nucleator Diaphanous can be seen by TIRF at the equatorial cortex in an anaphase S2 cell.** Actin-GFP (A) and Diaphanous-GFP and mCherry-tubulin (B) were visualized in *Drosophila* S2 cells during anaphase. Time 0 represents a time point in metaphase, and the later time points were acquired in anaphase. The more peripheral bands of actin-GFP are often seen in expressing cells and may be an artifact of overexpression. Diaphanous concentrates at the equatorial cortex shortly after microtubules begin stably interacting with the cortex. Bars, 10 µm.

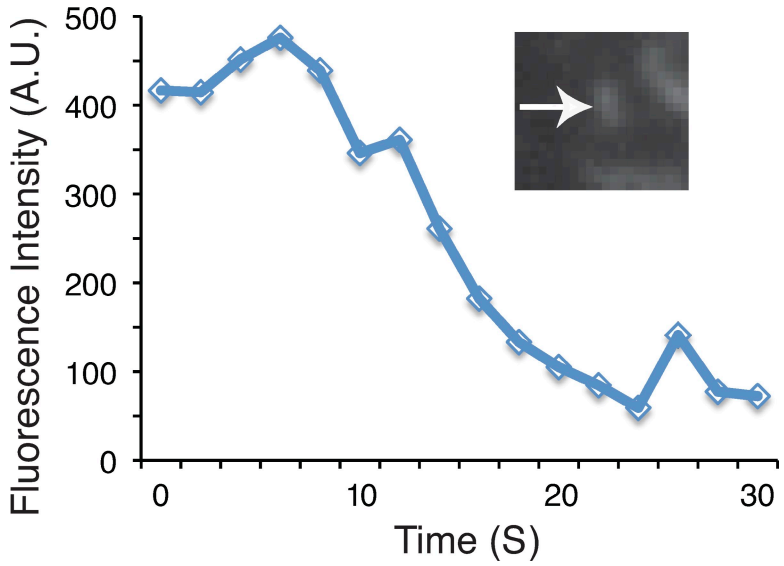

Figure S2. **Disappearance of myosin filaments from the polar cortex during anaphase.** A representative myosin particle (rodlike particle indicated by the arrow in the inset) is followed over time. Fluorescence intensity (7 × 7 pixel area surrounding the myosin particle) was measured over time and subtracted from a comparably size region of the cell devoid of myosin filaments. Myosin filament intensity is lost over several seconds. Arrow, 1 µm.

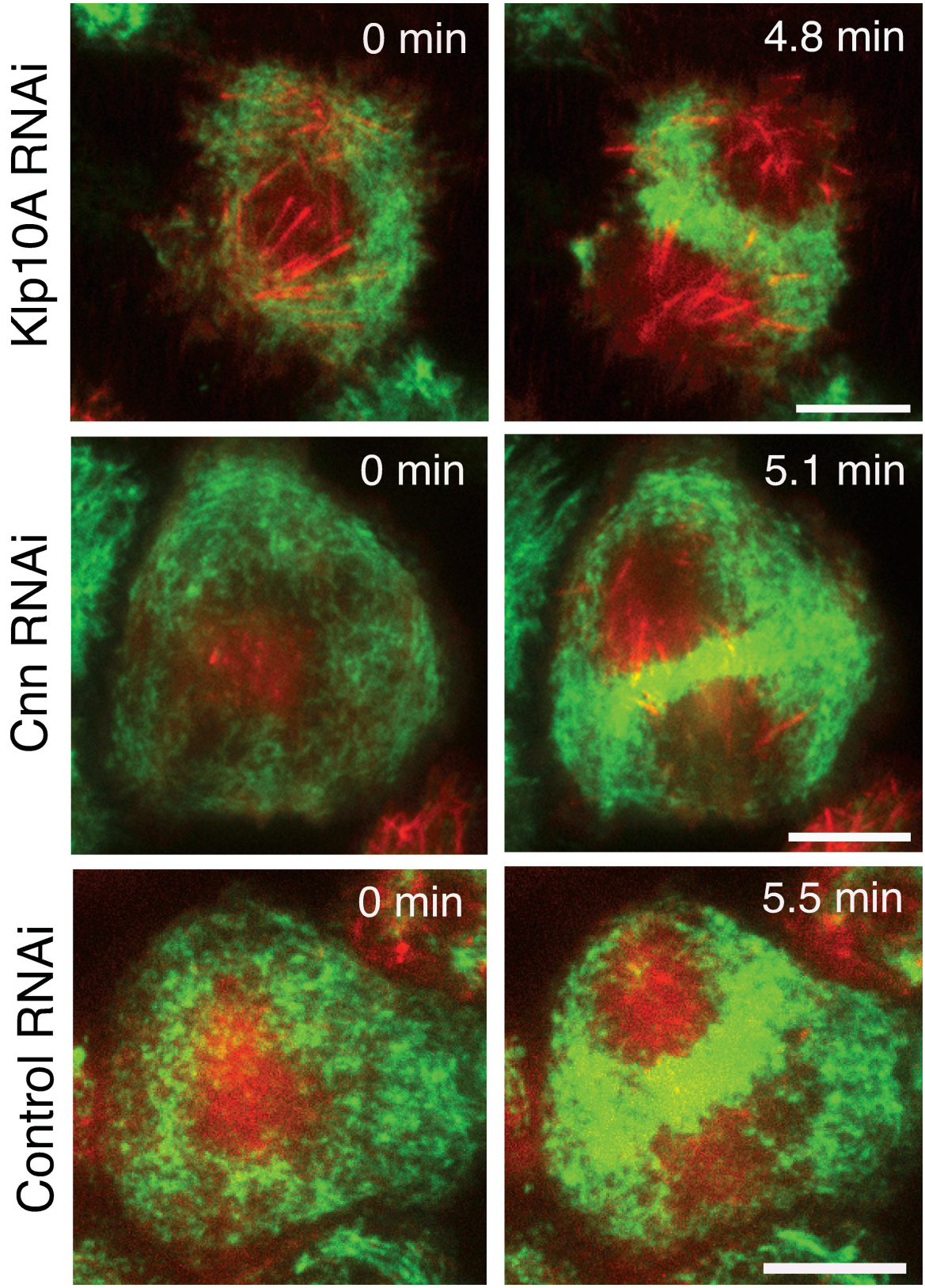

Figure S3. **Normal localization of myosin-GFP to the equator after RNAi depletion of Klp10A or centrosomin (Cnn).** A control RNAi (pBluescript) also is shown. Dual-color TIRF microscopy of mCherry-tubulin (red) and myosin-GFP (green). Time 0 represents a time point in metaphase, and the second time point was acquired in anaphase (accumulation of myosin at the equator). RNAi of Klp10A (a microtubule-destabilizing protein) results in the premature appearance of long, stable microtubules at the cell cortex before anaphase (compare microtubules at the 0 min time point with those in Fig. 2). RNAi of Cnn results in a drastic loss of astral microtubule that reach the polar cortex. See Video 3. Bars, 10 µm.

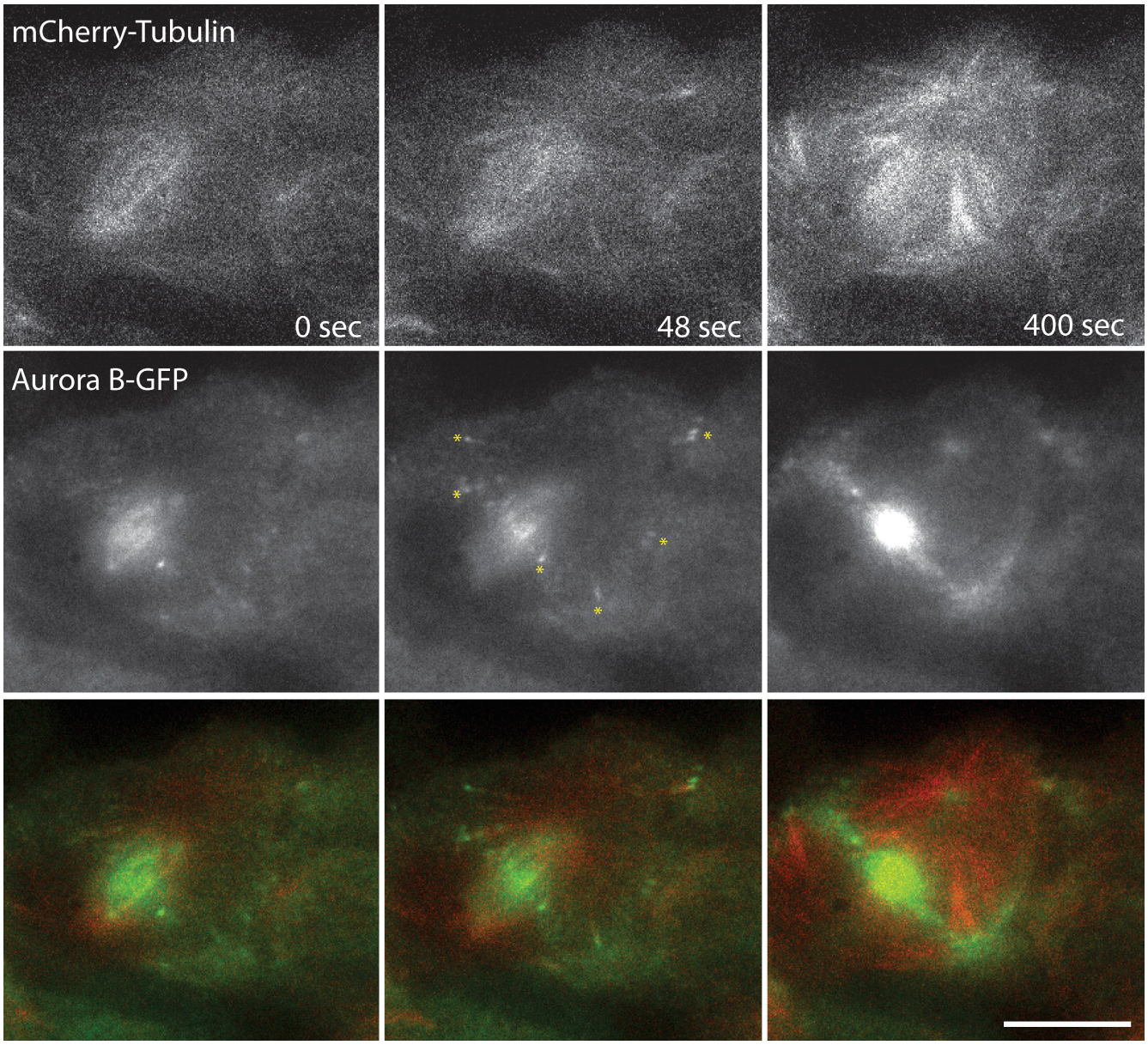

Figure S4. **Aurora B-GFP and microtubules at anaphase.** S2 cells stably expressing Aurora-B–GFP and mCherry-tubulin were imaged starting at the beginning of anaphase, with the laser illumination set near to but not achieving complete total internal reflection TIRF (allowing visualization of both the cortex and the deeper central spindle). Aurora B foci are found at the tips of microtubules at multiple sites at the cortex (several marked with asterisks) as well as a bright central region that is most likely the central spindle. See Video 7. Bar, 10 µm.

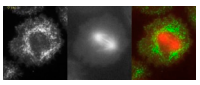

Video 1. **Time lapse of myosin-GFP (left, imaged by TIRF microscopy) and mCherry-tubulin (middle, imaged by epifluorescence; the spindle is close to the coverslip surface in this cell) during anaphase in a *Drosophila* S2 cell.** An overlay of the images is shown on the right. This video corresponds to the image in Fig. 1.

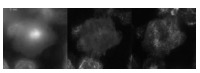

Video 2. **Time lapse of mCherry-tubulin by wide-field epifluorescence at the coverslip interface (left), mCherry-tubulin by TIRF (middle), and myosin-GFP by TIRF (right).** The acquisition of Cherry-tubulin by TIRF was at 2-s intervals, whereas the mCherry-tubulin by epifluorescence and myosin-GFP TIRF were at 36- and 10-s intervals, respectively. This video corresponds to the image in Fig. 3.

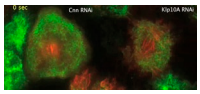

Video 3. **TIRF time lapse of myosin-GFP (green, images acquired every 10 s) and mCherry-tubulin (red, images acquired every 2 s) in a cell depleted of centrosomin (Cnn) by RNAi (left) and Klp10A (microtubule-depolymerizing Kinesin; right).** Despite drastically reducing microtubule nucleation from centrosomes after Cnn RNAi and increased microtubule stability after Klp10A RNAi, myosin relocation occurs in a manner similar to wild-type cells during anaphase. This video corresponds to the images in Fig. S3.

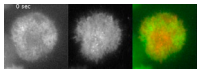

Video 4. **TIRF time lapse of myosin-GFP (left), mCherry-tubulin (middle), and overlay (myosin-GFP in green and mCherry-tubulin in red) in wild-type S2 cells from metaphase to anaphase.** This cell has many astral microtubules touching the cortex (within the TIRF illumination field) in the bottom left and very few in the top right. Despite this asymmetry (perhaps due to a tilting of the spindle), myosin localization occurs in a normal, symmetrical manner, and myosin clears from both poles.

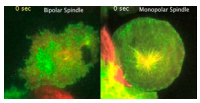

Video 5. **A comparison of Kinesin-6 anaphase dynamics in a cell with a bipolar or monopolar spindle.** (left) TIRF time lapse of Kinesin-6 (Pav-GFP; green) and mCherry-tubulin (red) in a wild-type S2 cell with a bipolar spindle from metaphase to anaphase. This video corresponds to the image in Fig. 4. (right) TIRF time lapse of Kinesin-6 (Pav-GFP; green) and mCherry-tubulin (red) in a cell with a monopolar spindle (S2 cells treated with dsRNA to Klp61F and BubR1). This video corresponds to the image in Fig. 5 B.

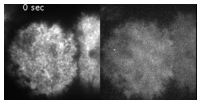

Video 6. **TIRF time-lapse imaging of myosin-GFP (left) and mCherry-tubulin (right) in an S2 cell depleted of Kinesin-6 (Pav) by RNAi.** Myosin-GFP localization to the equator and loss from the poles does not occur after RNAi Kinesin-6; microtubules tend to be more homogeneous throughout the cortex and less bundled. This video corresponds to the image in Fig. 3.

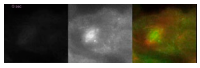

Video 7. **Time lapse of Aurora-B–GFP and microtubules at the metaphase-to-anaphase transition.** The laser illumination was set near to but not achieving complete total internal reflection TIRF to allow visualization of microtubules at the cortex as well as the more interior central spindle. Aurora B foci are seen at the tips of microtubules at multiple sites at the cortex as well as a bright central region (the central spindle). This video corresponds to the image in Fig. S4.

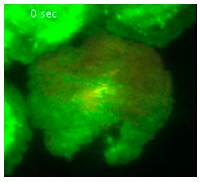

Video 8. **TIRF time-lapse imaging of EB1-GFP (green) and mCherry-tubulin (red).** EB1-GFP is seen on microtubule tips that grow to the cortex but does not accumulate on stable microtubule bundles at the equator, in contrast to Kinesin-6 (see Video 5).

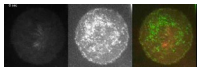

Video 9. **TIRF time lapse of mCherry-tubulin (left), myosin-GFP (middle), and overlay (myosin in green and tubulin in red; right) in a cell with a monopolar spindle from metaphase to anaphase (cell was depleted of Klp61F [Kinesin-5] and BubR1 by RNAi).** This video corresponds to the image in Fig. 5 A.

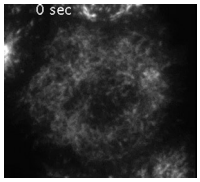

Video 10. **TIRF time lapse of myosin-GFP in a cell with a symmetric monopolar spindle from metaphase to anaphase (cell was depleted of Klp61F [Kinesin-5] and BubR1 by RNAi).** At anaphase, myosin-GFP concentrates at the cell perimeter and becomes depleted from the central regions of the adhered cortex. Slowly, myosin breaks symmetry and ultimately relocalizes to the middle. This video corresponds to the image in Fig. 6.